Journal of Marine Science and Application (2019) 18:48–53
https://doi.org/10.1007/s11804-019-00070-0

RESEARCH ARTICLE

Hydrodynamic Simulation of Wave Energy Converter Using Particle-Based Computational Fluid Dynamics

Yodchai Tiaple[1]

Received: 12 October 2017 / Accepted: 27 April 2018 / Published online: 8 February 2019

Abstract
Wave energy from the ocean is currently a very popular renewable energy, and its development has primarily focused on the shape of the wave energy converter (WEC) used to efficiently convert wave energy into electrical energy. However, the free surface ocean wave problem is very complex and the parameters affecting WEC behavior are difficult to understand. In this paper, based on the Lattice-Boltzmann method, we present particle-based CFD simulation results for the pivoted-type WEC that exhibits both vertical and horizontal motions. In this method, the computation domain need not be a mesh and complex geometry is not a limiting factor. Using a free-surface turbulence model, we simulated the fluid–structure interaction. We detail our simulation results, which show good agreement with those in the literature.

Keywords Wave energy converter · Pivoted buoy · Lattice–Boltzmann · Particle-based · CFD

1 Introduction

Wave energy is a renewable energy that is gaining the attention of researchers around the world, due to the growing interest in studying how to use energy from the sea to generate electricity. Wave energy is a high-density energy source compared with other renewable energy sources (Clément et al., 2002). The entire world is estimated to have around 2 700 GW in energy resources, but only 500 GW can be exploited using today's technologies (*McCormick* et al. 2009).

Wave energy converter (WEC) technology has been widely used to extract energy from ocean waves. To date, WECs have been developed and demonstrated in more than 100 pilot studies around the world (Kempener and Neumann 2014). The four types of WEC are classified according to the operating system used: oscillating water column (OWC), overtopping devices, wave-activated bodies (point absorbers and wavelength absorbers), and unclassifiable (Kelly 2007). Many researchers are interested in modeling the floating point absorber, which is believed to be the most cost-effective technology for absorbing wave energy (Ye and Yi-Hsiang 2012).

Point absorber models consist of a set of horizontal buoys with lengths shorter than the incident wavelength. The buoys move up and down either in one direction or with more degrees of freedom. The wave energy is then captured by damping the buoy movement (Griet De Backer 2009) and is then converted to electrical power by a power takeoff (PTO) system (Drew et al. (2009), Mueller (2007), Plummer and Schlotter (2009), Xiao C (2014), Choi et al. (2012)). Examples of the surging-type point absorber include the WRASPA (Bhinder et al. 2009) and OSWEC (Yu et al. 2015), of the heaving-type include the Manchester Bobber (Lok 2010) and HPAs (van den Berg et al. 2010), and of the pitching-type include the Salter duck (Salter et al. 1976) and bioWAVE (Gonzalez et al. 2009). The model parts can be multi-directional, such as in the Wavestar (Marquis et al. 2012) and DEXAWAVE (Zanuttigh et al, 2013), or pivoted Coiro et al. (2016).

In this study, we focus on the pivoted WEC, which is described in detail in the experimental and simulation reports of

Article Highlights
- A particle-based CFD based on the Lattice–Boltzmann method allows there to be no limitation on the complexity of the model and is also suitable for moving model.
- The hydrodynamic simulations for the pivoted WEC can predict its performance which is consistent with the experimental results reported in the literature.
- The energy conversion efficiency of the pivoted floating buoy is quite high compared to with the pure heave motion of the WEC.

✉ Yodchai Tiaple
yodchai.ti@ku.th

[1] Department of Maritime Engineering, Faculty of International Maritime Studies, Kasetsart University, Sriracha Campus, Chonburi 20230, Thailand

Coiro et al. (2016). The pivoted WEC utilizes the commercial CFD simulation XFlow and a particle-based approach based on the Lattice–Boltzmann method (Holman et al. 2012).

2 Theory

Wave energy is the sum of the kinetic and potential energies per unit area of sea surface, which is expressed as the specific energy or energy density ($\overline{E}$) as follows (Yodchai Tiaple et al. 2013):

$$\overline{E} = \underbrace{\frac{1}{16}\rho g H^2}_{\text{K.E.}} + \underbrace{\frac{1}{16}\rho g H^2}_{\text{P.E.}} = \frac{1}{8}\rho g H^2 \quad (\text{J/m}^2) \tag{1}$$

where ρ is fluid density (kg/m^3), g is gravitational acceleration (m/s^2), and H is wave height (m).

The average energy per unit area of a wave traveling at a wave group velocity C_g is called the energy flux or wave power ($\overline{P}$), which is expressed as follows (Hamid Sarlak et al. 2010):

$$\overline{P} = \overline{E}\cdot C_g \approx \frac{1}{8}\frac{\rho g H^2 \lambda_n}{T} \quad (\text{W/m}) \tag{2}$$

where λ_n is wavelength (m) and T is the wave period (s).

A pivoted floating buoy oscillates in vertical (heave) and horizontal (surge) modes or in a pure pitch mode on the wave surface in response to excitation from incoming waves (see Fig. 1). The equation for buoy motion in the pitch direction is as follows (Coiro et al. 2016):

$$I\ddot{\theta} + B\dot{\theta} + K\theta = M_{\text{ext}} + M_{\text{PTO}} \tag{3}$$

where I is the pitch mass moment of inertia and added inertia of floater, B is damping coefficient, K is hydrostatic restoration stiffness coefficient, M_{ext} is the moment due to incident and diffracted waves, and M_{PTO} is the moment due to the point pivoted PTO.

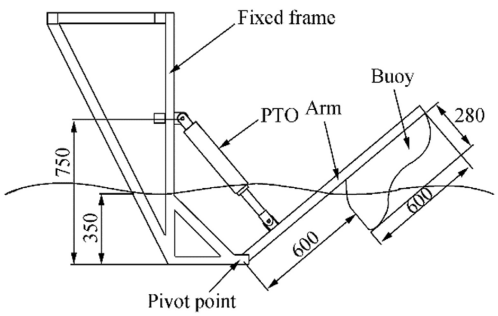

Fig. 1 Schematic of pivoted floating buoy

The M_{PTO} value is obtained from the PTO system, which is primarily an actuator that generates a force in proportion to the velocity, as expressed by the following equation (Coiro et al. 2016):

$$M_{\text{PTO}} = \boldsymbol{F}\cdot r = K\boldsymbol{V}\cdot r \tag{4}$$

where K is the proportionality coefficient and r is the distance from the pivot point to the position of the actuator.

3 Numerical Approach

Particle-based methods have been developed based on the Lattice–Boltzmann method (LBM), which was developed to simplify the mesh process of the traditional CFD. The LBM allows there to be no limitation on the complexity of the model and is also suitable for models with moving parts. The LBM use statistical distribution functions f_i with real variables. The Boltzmann transport equation is as follows (Next Limit Dynamics SL, 2016a):

$$\frac{\partial f_i}{\partial t} + e_i\cdot\nabla f_i = \Omega_i, i = 1, ..., b \tag{5}$$

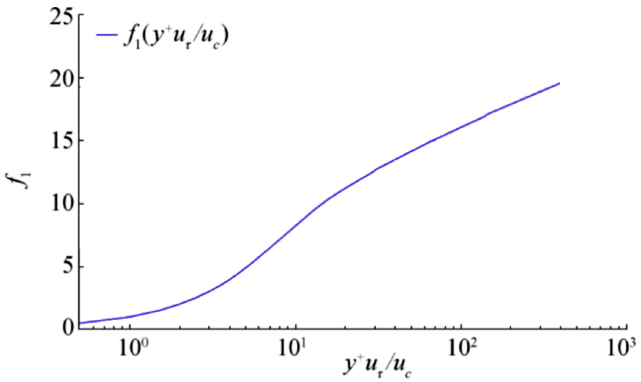

(a) Interpolating function f_1

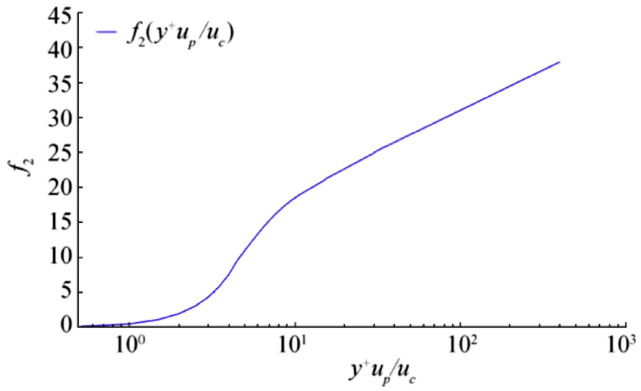

(b) Interpolating function f_2

Fig. 2 Unified wall laws (Holman et al. 2012)

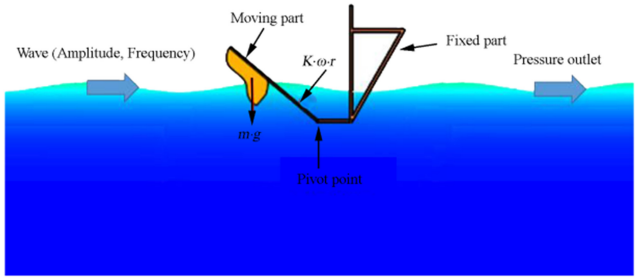

Fig. 3 Force acting on pivoted buoy and boundary condition

where f_i is the particle distribution function in the direction i, e_i is the discrete velocity in the direction i, and Ω_i is the collision operator.

Ω_i is based on the multiple-relaxation-time (MRT) collision operator in central moment space, which is defined as follows (Next Limit Dynamics SL, 2016b):

$$\Omega_i^{\mathrm{MRT}} = M_{ij}^{-1}\hat{S}_{ij}(m_i^{\mathrm{eq}} - m_i) \tag{6}$$

where $\hat{S}_{ij}$ is the diagonal of the collision matrix, m_i^{eq} is the equilibrium of the moment m_i, M_{ij} is the transformation matrix.

The central moment can be defined as follows:

$$\tilde{\mu}_x k_y t_z m = \sum_i^N f_i (e_{ix} - u_x)^k \left(e_{iy} - u_y\right)^l (e_{iz} - u_z)^m \tag{7}$$

The large eddy simulation (LES) for turbulence modeling is called the wall-adapting local eddy (WALE) viscosity model, which is expressed as follows (Next Limit Dynamics SL, 2016a):

$$v_t = \Delta_f^2 \frac{\left(G_{\alpha\beta}^d G_{\alpha\beta}^d\right)^{3/2}}{\left(S_{\alpha\beta}S_{\alpha\beta}\right)^{5/2} + \left(G_{\alpha\beta}^d G_{\alpha\beta}^d\right)^{5/4}} \tag{8}$$

$$S_{\alpha\beta} = \frac{g_{\alpha\beta} + g_{\alpha\beta}}{2} \tag{9}$$

$$G_{\alpha\beta}^d = \frac{1}{2}\left(g_{\alpha\beta}^2 + g_{\beta\alpha}^2\right) - \frac{1}{3}\delta_{\alpha\beta} g_{\gamma\gamma}^2 \tag{10}$$

$$g_{\alpha\beta} = \frac{\partial u_\alpha}{\partial x_\beta} \tag{11}$$

$$\Delta_f = C_w \Delta x, \quad C_w \approx 0.325 \tag{12}$$

A generalized wall law is used as the boundary layer condition, which includes the effect of adverse and favorable pressure gradients:

$$\frac{U}{u_c} = \frac{U_1 + U_2}{u_c} = \frac{u_\tau U_1}{u_c\, u_\tau} + \frac{u_p U_2}{u_c\, u_p} \tag{13}$$

$$= \frac{\tau_w\, u_\tau}{\rho u_\tau^2 u_c} f_1\left(y^+ \frac{u_\tau}{u_c}\right) + \frac{\mathrm{d}p_w/\mathrm{d}x}{|\mathrm{d}p_w/\mathrm{d}x|}\frac{u_p}{u_c} f_2\left(y^+ \frac{u_p}{u_c}\right) \tag{14}$$

$$y^+ = \frac{u_c y}{v} \tag{15}$$

$$u_c = u_\tau + u_p \tag{16}$$

$$u_\tau = \sqrt{|\tau_w|/\rho} \tag{17}$$

$$u_p = \left(\frac{v}{\rho}\left|\frac{\mathrm{d}p_w}{\mathrm{d}x}\right|\right)^{1/3} \tag{18}$$

Functions f_1 and f_2 are shown in Fig. 2 (Holman et al. 2012).

4 Simulation Setup

Figure 1 shows a schematic of a pivoted buoy, for which the arm length is 0.6 m and the width of the buoy is 1 m. The buoy weighs 32.5 kg and its draught is 0.2 m. We imported the model into the Xflow program, with a domain length of 12 m, width of 5 m, and depth of 3 m.

We defined the inlet condition using a linear wave function, as expressed in the following equation (Next Limit Dynamics SL, 2016b):

$$v_x = v_w + \frac{A\omega}{\sinh kh}\cosh k(h+y)\sin(\omega t - kx) \tag{19}$$

$$v_y = \frac{A\omega}{\sinh kh}\sinh k(h+y)\cos(\omega t - kx) \tag{20}$$

Table 1 Lattice resolution of each zone

	Resolution/*m*	No. of element at *t* = 3 s
x	0.2	13 078
$x/2$	0.1	38 754
$x/2^2$	0.05	164 783
$x/2^3$	0.025	686 882
$x/2^4$	0.0125	2 706 892

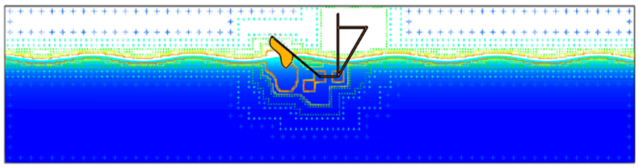

Fig. 4 Lattice structure of the domain

where x is the horizontal position, y is the vertical position, t is time, ω is the angular velocity ($\omega = 2\pi f$), h is depth, and k is the wave number, as defined by the following equation:

$$\omega^2 = gk\tanh(kh) \tag{21}$$

Using rigid body dynamics, we defined the pivoted buoys having a weight of 32.5 kg and moving in the pitch mode around the pivot, with a gravitational force equal to 32.5 × 9.81 N acting at the center of gravity of the buoy. The momentum from the actuator has a force equal to $K \cdot (\omega \cdot r)$ acting on the buoy's arm at position 0.27 m. We obtained the ω by the movement of the buoy by the incident wave, as shown in Fig. 3.

The XFlow program is a particle-based method, so there is no need to address any meshing process. It is possible to construct a lattice structure by defining the resolutions for the outer, inner, and wake geometries. The lattice structure can be automatically divided into lattice density zones.

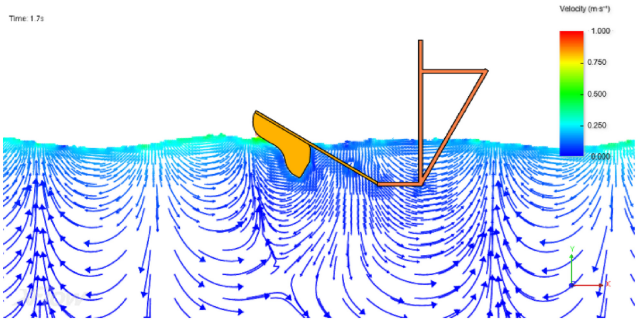

(a) Lowest position

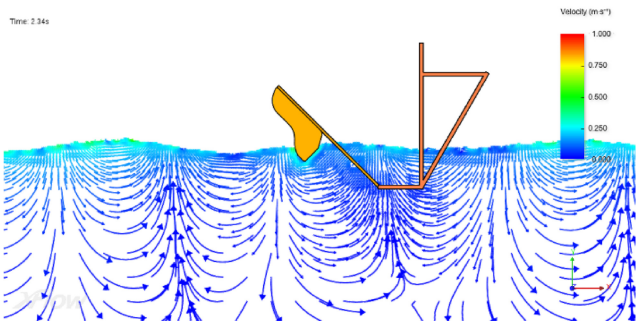

(b) Maximum position

Fig. 5 Positions of the pivoted buoy

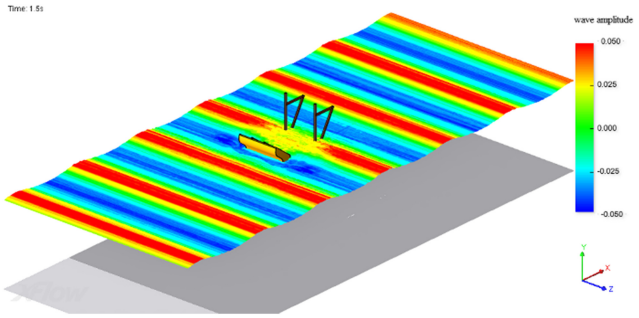

Fig. 6 3D free surface at $t = 1.5$ s.

Table 1 shows the lattice resolution of each zone and Fig. 4 shows the lattice structure in the computational domain.

5 Results

In the simulations, we set the wave amplitude (A) to 5 cm and the frequencies (f) to 0.7 Hz, 0.8 Hz, and 0.9 Hz. The buoyancy weight is 32.5 kg and the force generated by the PTO is equal to $\boldsymbol{KV}$ for a radius 0.27 m from the pivot point. The K value varies according to the simulation parameters.

Figure 5a shows the buoy in the lowest position, and Fig. 5b shows the buoy in the maximum position for a frequency = 0.9 Hz, and K= 360 Ns·m^{-1}. Figure 6 shows the wave free surface at *1.5* s.

The power generated from the buoy can be calculated as follows:

$$P = -T{\cdot}\omega = -(F \times r){\cdot}\omega = -((K{\cdot}V) \times r){\cdot}\omega \tag{22}$$

Figure 7 shows the power output from the buoys versus time for a wave amplitude = 5 cm, frequency = 0.8 Hz, and $K = 600$ Ns·m^{-1}.

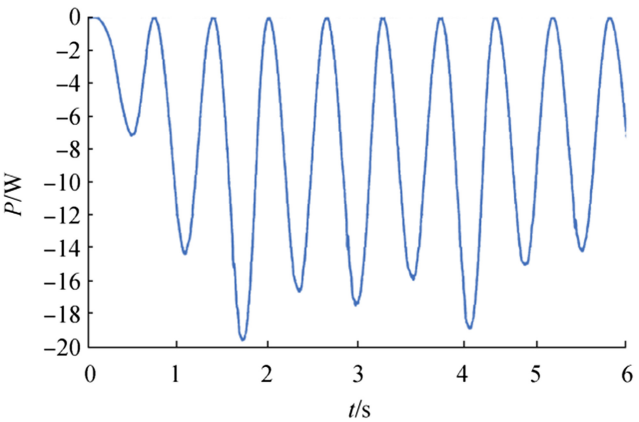

Fig. 7 Instantaneous power time history ($A = 0.05$ m, $f = 0.8$ Hz, $K = 600$ Ns·m^{-1})

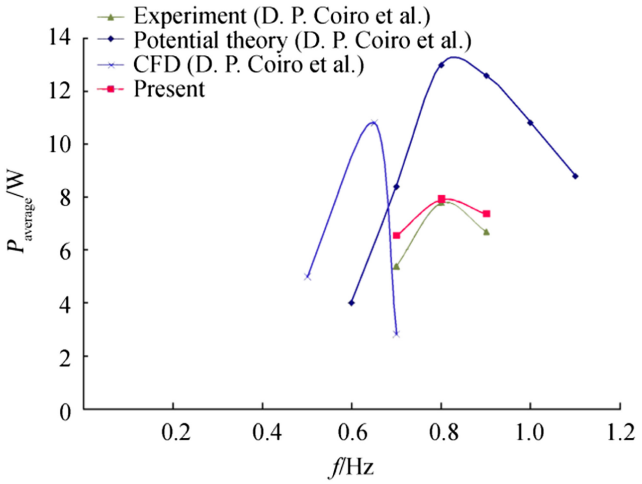

Fig. 8 Average power for $A = 5$ cm and $K = 600$ Ns·m^{-1}

Figure 8 shows the average power at a wave amplitude of 5 cm, $K = 600$ Ns·m^{-1}, and frequencies of 0.7 Hz, 0.8 Hz, and 0.9 Hz, which are comparable with the results reported by Coiro et al. (2016). In the figure, we can see that the numerical values closely resemble the experimental results.

Next, we compared the energy produced with the wave energy, which is known as the capture width ratio (CWR), as follows (Coiro et al. 2016):

$$\mathrm{CWR} = \frac{P_{\mathrm{avg}}}{P_{\mathrm{wave}} \cdot B} = 0.66 \tag{23}$$

where B is the buoy width and P_{avg} is the average power produced. This indicates the energy conversion efficiency of the buoy device.

For cases in which the wave amplitude is 5 cm and the frequency is 0.8 Hz, the P_{wave} is about 12 W. From the simulation, we found the P_{avg} to be 7.9 W, so the CWR is 0.66, which is quite high compared with the pure heave motion of the WEC (Kalofotias 2016).

Figures 9, 10 and 11 compare the powers determined by our simulations and the experimental results reported by Coiro et al. (2016) for a wave amplitude = 5 cm and frequencies = 0.7, 0.8, and 0.9, respectively. The results show our simulated results to be consistent with the experimental results.

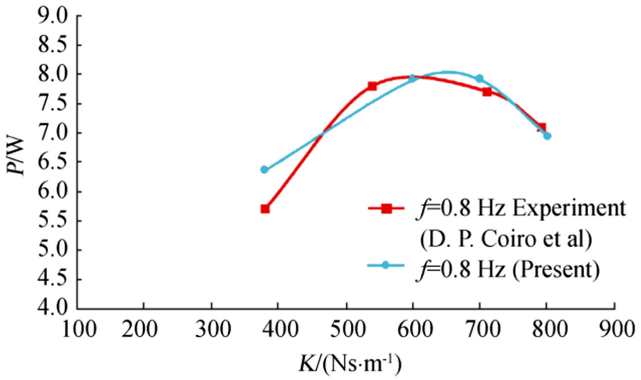

Fig. 10 Power for $A = 5$ cm and $f = 0.8$ Hz

6 Conclusions

In this study, we performed particle-based CFD simulations based on the Lattice–Boltzmann method, which reduces the meshing process and the complexity constraints of the geometric model used in the traditional CFD simulation. Using this modeling approach, simulating challenging scenarios becomes easier, especially regarding the problem of free surface waves that have a fluid–structure interaction. Our results confirmed that the hydrodynamic simulation of a pivoted buoy can accurately monitor its behavior and predict its performance. The simulation results are consistent with the experimental results reported in the literature. Therefore, we can conclude that particle-based CFD simulations have high accuracy and reliability and can be used as an engineering tool for analysis and design.

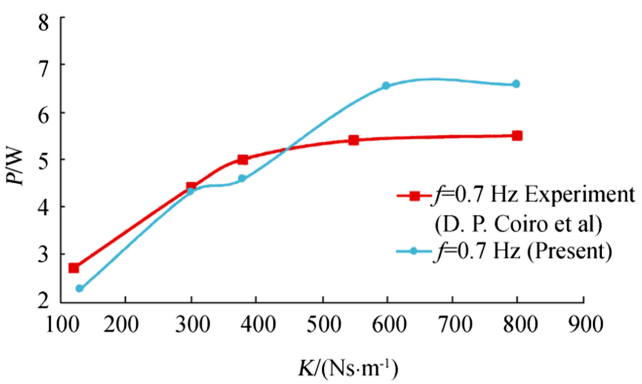

Fig. 9 Power for $A = 5$ cm and $f = 0.7$ Hz

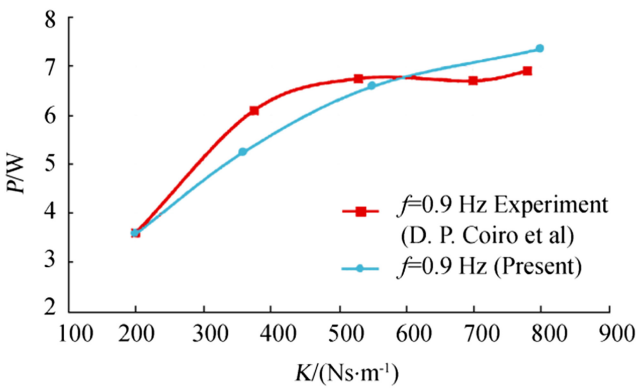

Fig. 11 Power for $A = 5$ cm and $f = 0.9$ Hz

Funding Information The project is sponsored by the Energy Policy and Planning Office, Ministry of Energy, Thailand (Contract No. 07-02-57-014).

References

Bhinder MA, Mingham CG, Causon DM, Rahmati MT, Aggidis GA, Chaplin RV (2009) Numerical modelling of a surging point absorber wave energy converter. *Proceedings of the 8th European Wave and Tidal Energy Conference*, Uppsala, Sweden. https://doi.org/10.1115/OMA2009-79392

Choi K-S, Yang D-S, Park S-Y, Cho B-H (2012) Design and performance test of hydraulic PTO for wave energy converter. *Int J Precis Eng Manuf* **13**(5):795–801. https://doi.org/10.1007/s12541-012-0105-4

Clément AH, McCullen P, Falcão A, Fiorentino A, Gardner F, Hammarland K, Lemonis G, Lewis T, Nielsen K, Petroncini S, Pontes MT, Schild P, Sjöström BO, Sorensen HC, Thorpe T (2002) Wave energy in europe: current status and perspectives. *Renew Sust Energ Rev* 6:405–431. https://doi.org/10.1016/S1364-0321(02)00009-6

Coiro DP, Troise G, Calise G, Bizzarrini (N (2016) Wave energy conversion through a point pivoted absorber: Numerical numerical and experimental tests on a scaled model. Renew Energy:317–325. https://doi.org/10.1016/j.renene.2015.10.003

Drew B, Plummer AR, Sahinkaya MN (2009) A review of wave energy converter technology. Proc. IMechE, Part A: *J. Power and Energy*. https://doi.org/10.1243/09576509JPE782

Gonzalez CA, Kloos G, Finnigan T (2009) Development of a multi-bladed 250 kW pitching wave-energy converter. *Proceedings of the 8th European Wave and Tidal Energy Conference*, Uppsala, Sweden.

Griet De Backer (2009) Hydrodynamic design optimization of wave energy converters consisting of heaving point absorbers, Doctor Dissertation, Ghent University, Belgium. www.vliz.be/imisdocs/publications/220173.pdf

Holman DM, Brionnaud RM, Abiza Z (2012) Solution to industry benchmark problems with the lattice-Boltzmann code XFlow, *ECCOMAS*.

Ka Sing Kane Lok, 2010. Optimisation of the output of a heaving wave energy converter, PhD thesis, University of Manchester.

Kalofotias F (2016) Study for the hull shape of a wave energy converter-point absorber. Master thesis, University of Twente, Netherlands.

Kelly S (2007) Hydrodynamic optimisation of a point wave- energy converter using laboratory experiments, Thesis, The University of Auckland, New Zealand.

Marquis L, Kramer MM, Kringelum J, Chozas JF, Helstrup NE (2012) Introduction of wavestar wave energy converters at the Danish offshore wind power plant Horns Rev 2. *4th International Conference on Ocean Energy*, 17 October, Dublin.

McCormick ME, Ertekin CR (*2009*) *Renewable sea power: waves, tides, and thermals new research funding seeks to put them to work for us. ASME Mech Eng* ***131****(5):36–39*. https://doi.org/10.1115/1.2009-MAY-4

Mueller MA, Henk Polinder, Nick Baker (2007) Current and novel electrical generator technology for wave energy converters, *2007 IEEE International Electric Machines & Drives Conference*, 1401–1406. https://doi.org/10.1109/IEMDC.2007.383634

Next Limit Dynamics SL, 2016a. *XFlow 2016 Theory guide*.

Next Limit Dynamics SL, 2016b. *XFlow 2016 User guide*.

Plummer AR, Schlotter M (2009) Investigating the performance of a hydraulic power take-off. *Proceedings of the 8th European Wave and Tidal Energy Conference*, Uppsala, Sweden.

Ruud Kempener, Frank Neumann (2014) Wave energy technology brief. *IRENA Ocean Energy, Technology Brief 4*.

Salter SH, Jeffery DC, Taylor JRM (1976) The architecture of nodding duck wave power generators. *Nav Archit* 1:21–24

Sarlak H, Seif MS, Abbaspour M (2010) Experimental investigation of offshore wave buoy performance. *Journal of Marine Engineering*, **6**(11), Spring & Summer.

Van den Berg J, Ricci P, Santos M, Rico A, Lopez J (2010) Hydrodynamic performance of heaving wave energy converters in wave climates. *3rd International Conference on Ocean Energy*, 6 October, Bilbao.

Xiao Cui (2014) Study of power decoupling properties of hydraulic power take-off system in ocean wave converter. *2014 4th International Conference on Future Environment and Energy*, IPCBEE. https://doi.org/10.7763/IPCBEE. *2014. V61*. 18

Li Ye, Yu Yi-Hsiang (2012) A synthesis of numerical methods for modeling wave energy converter-point absorbers. National Renewable Energy Laboratory (NREL), NREL/JA-5000-52115

Yodchai Tiaple, Surasak Phoemsapthawee, Phansak Iamraksa, Wanlee Noenmosi, Nontiphat Taweewat (2013) Study and research to develop wave energy converter for Thailand, Report (in Thai).

Yu YH, Jenne DS, Thresher R, Copping A, Geerlofs S, Hanna LA (2015) Oscillating surge wave energy converter, Technical Report, National Renewable Energy Laboratory (NREL), January.

Zanuttigh B, Angelelli E, Kofoed JP (2013) Effects of mooring systems on the performance of a wave activated body energy converter. *Renew Energy* 57:422–431. https://doi.org/10.1016/j.renene.2013.02.006